Hydrosphere, 2026, 1: 9380005-VR
https://doi.org/10.26599/HYD.2023.9380005.VR
Research Article

Blue water: Its distribution and relationship to the river network [version of record]

Chensong Zhao[1,2,3], Yu Zhang[1,2,3], Deyu Zhong[1,2,3,4,✉], Guangqian Wang[1,2,3]

[1]*State Key Laboratory of Hydroscience and Engineering, Tsinghua University, Beijing 100084, China*
[2]*Key Laboratory of Hydrosphere Sciences of the Ministry of Water Resources, Tsinghua University, Beijing 100084, China*
[3]*Department of Hydraulic Engineering, Tsinghua University, Beijing 100084, China*
[4]*Joint-Sponsored State Key Laboratory of Plateau Ecology and Agriculture, School of Water Resources and Electric Power, Qinghai University, Xining 810016, China*

ABSTRACT
Blue water, which includes freshwater in reservoirs, lakes, rivers, and aquifers, plays a crucial role in sustaining life on Earth and serves as a direct water resource for human societies. The distribution of blue water resources shows spatiotemporal variations, making it important to comprehensively understand the distribution patterns and influencing factors of blue water resources in river basins. In this study, the normalized runoff was analyzed using methods including stationarity testing, correlation analysis, and variance analysis to explore its spatiotemporal patterns and the relationships with river structure. The results indicate that the normalized runoff time series show stationarity at a global scale and show correlations with river network density and the distance to the nearest downstream sink, but the strength of these correlations varies across different regions on different continents. The normalized runoff also shows variations among river order. Further research could examine predicting blue water availability given information on river network structure and climate.

KEYWORDS
Blue water, water distribution, runoff, river structure.

1 Introduction

Climate change and human activities have caused widespread impacts, altering terrestrial and freshwater ecosystems globally while also affecting water security (Lee et al., 2023). This exacerbates the blue water crisis blue water refers to fresh surface water and groundwater found in reservoirs, lakes, rivers, and aquifers (Falkenmark et al., 2006). It plays a crucial role in sustaining life on Earth and serves as a direct water resource for human society. However, the availability of blue water shows significant spatiotemporal heterogeneity in terms of per capita and total quantity (Shiklomanov, 2000; Mekonnen & Hoekstra, 2016; Jaramillo & Destouni, 2015). Therefore, the distribution of blue water resources has significant implications for ecosystem, agricultural production, and the sustainable development of human society. A comprehensive understanding of the distribution patterns of blue water resources in river basins and their influencing factors is essential for achieving sustainable use of water resources.

Earlier studies on the spatial distribution of blue water resources have chosen to compare river basins found in different regions to understand the differences in their distribution, and thereby reveal variations in water resource carrying capacity and the potential for sustainable use across different regions (Arnell, 2004; Huang et al., 2017). Some studies have also conducted comparative analyses of multiple sub-basins within a large river basin to reveal the spatial distribution of water resources within the river basin (Liu et al., 2022). However, due to the spatiotemporal heterogeneity of blue water resource distribution, previous research has paid limited attention to conducting comprehensive comparative studies on the distribution of blue water resources among sub-basins within different river basins at a finer scale.

Earlier studies have examined the influencing factors of spatial distribution of blue water resources by analyzing the effects of geographical and climatic factors, revealing differences among different river basins. Factors such as topography (Wang et al., 2018), soil type (Scanlon et al., 2007), and vegetation cover (Zhang et al., 2001; Feng et al., 2016) play a crucial role in the distribution of blue water resources. Additionally, climate change also affects the spatial distribution of blue water resources, including changes in precipitation patterns and evapotranspiration (Kundzewicz et al., 2008; Döll et al., 2018; IPCC, 2023). Expanding upon the earlier research, we should consider the influence of rivers on blue water resources. Rivers play a pivotal role in hydrological systems within river basins (Falkenmark et al., 2006). They significantly influence the transport and distribution of blue water resources. Additionally, river discharge contributes significantly to renewable freshwater resources (Oki et al., 2006). River structure refers to the physical morphology and characteristics of rivers within their river basins, including physical parameters of river channels, riverbed shapes, bank features, and other related geomorphic attributes (Twidale, 2004). It describes the geometric shape and geographical distribution of rivers, reflecting their hydraulic characteristics and geomorphological evolution (Leopold et al., 1964). Exploring the relationship between river structure and the distribution of blue water resources contributes to a more comprehensive understanding of blue water resource dynamics, enabling informed decision-making and sustainable management in the face of climate change.

In the composition of blue water resources, runoff assumes a primary and paramount role (Shiklomanov et al., 2003). The aim of this study is to analyze the runoff effects of river structure. Through the analysis of normalized runoff time series, the stationarity of normalized runoff is explored. By analyzing the correlation between normalized runoff and river structure parameters, such as river network density,

✉Address correspondence to Deyu Zhong, zhongdy@tsinghua.edu.cn

we will compare the differences in runoff effects of river structures among sub-basins within different river basins at a finer scale. This study will also analyze the variability of runoff between river orders in different areas. By conducting a comprehensive analysis of river orders and comparing the runoff effects of river structure within different river basins in different regions, we can gain a better understanding of the distribution patterns of blue water resources in different regions.

2 Data and methods

In this study, the normalized runoff from various river basins around the world was analyzed for stationarity testing and correlation with river structure parameters. Analysis of variance (ANOVA) was also conducted for normalized runoff of different river orders.

2.1 Geographical delineation of basins

The analyses in this study are based on the geographic delineation of river basins from the HydroBASINS dataset (Lehner et al., 2013). HydroBASINS presents sub-basin boundaries on a global scale and provides 12 hierarchically nested sub-basin delineations based on the Pfafstetter codes on a global scale. The Pfafstetter coding system was selected for this study because it provides a globally consistent, topology-based hierarchical framework that uniquely identifies each sub-basin within a drainage network (Verdin & Verdin, 1999). Unlike alternative coding systems such as the Hydrologic Unit Code (HUC) used in the United States, which is region-specific, or simple sequential numbering systems, Pfafstetter coding inherently preserves hydrological connectivity and drainage hierarchy through its algorithmic structure (Olivera et al., 2002). This makes it particularly suitable for global-scale comparative analyses of river structure effects on runoff distribution, as the coding itself reflects the topological position of each sub-basin within the larger watershed system. Considering the resolution of the runoff data, the first seven levels of sub-basin delineation were used in this study. The first three levels of Pfafstetter codes in HydroBASINS were assigned manually. Level 1 distinguishes 9 continental regions including Africa, Arctic, Asia, Australasia, Europe and the Middle East, Greenland, North and Central America, South America, and Siberia. Level 2 further subdivides each region into large sub-units according to the distribution of river basins. And at Level 3, the largest river basins of each region start to break out. Figure 1 shows the division results for Level 1 and Level 3. From Level 4 onwards, the breakdown follows the traditional Pfafstetter coding (Lehner et al., 2013).

2.2 River information and normalized runoff extraction

River structure data for this study were obtained from the HydroRIVERS dataset (Lehner et al., 2013). HydroRIVERS is a vectorized line network of all global rivers that have a catchment area of at least 10 km² or an average river flow of at least 0.1 m³/s, or both. HydroRIVERS includes information on some of the attributes of the river, such as the river reach length, the distance from upstream headwaters and ocean outlet, the river order, and an estimate of long-term average discharge. By searching the Pfafstetter code, it is possible to find the corresponding river basin for each river network. Since a single river basin may correspond to multiple rivers, information on attributes available for rivers, such as rivers reach length and catchment area, is accumulated to obtain information on the overall river structure of the river basin. The runoff time series data used in this study are from the ERA5-Land dataset (Muñoz Sabater, 2019). The data are monthly averages with a temporal range of 2013–2022 and a spatial resolution of 0.1°, standing for runoff depth (R) in m. The runoff corresponded to the river basin to obtain the surface-averaged runoff depth of the river basin. The analysis in this paper does not cover Greenland because a valid basin-runoff correspondence could not be extracted in Greenland. For each month's data, the largest runoff depth $R_{\max}$ and the smallest runoff depth $R_{\min}$ are obtained by considering all runoff time series data for each large basin (with the same Pfafstetter code's first three digits). The MinMax normalization is then applied to all the runoff time series data, as Eq. (1):

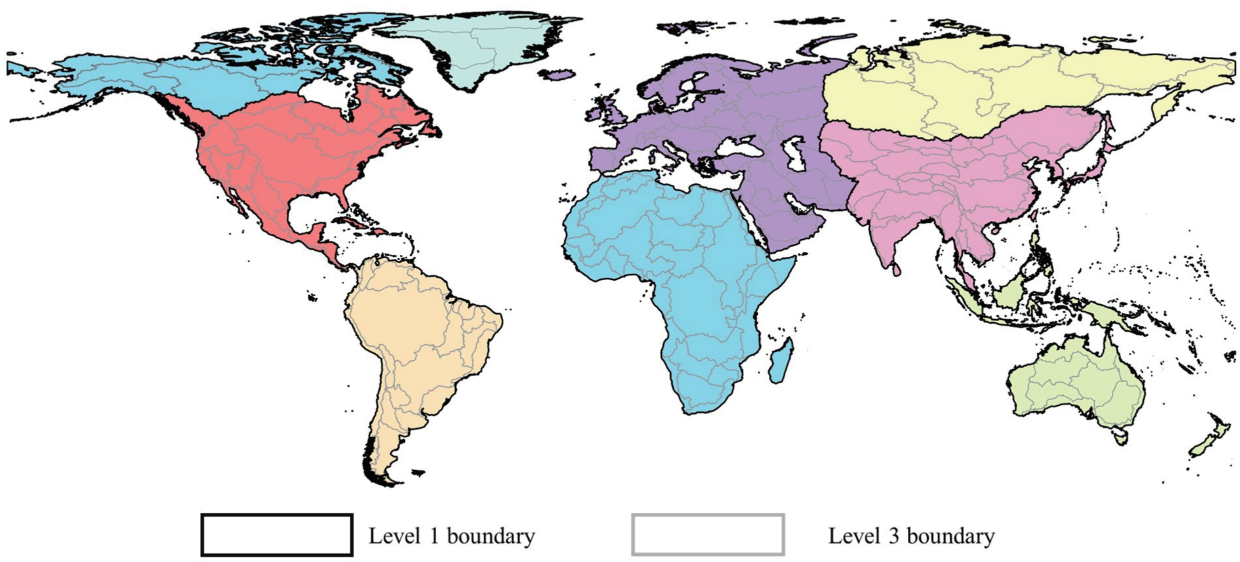

Fig. 1 The geographic delineation of river basins. Level 1 is distinguished by different colors. The thick black solid line is its boundary. The corresponding region for each Level 1 is divided into multiple Level 3 distinct regions representing different large river basins. Region boundaries are delineated by solid gray lines.

$$R = \frac{R - R_{\min}}{R_{\max} - R_{\min}} \tag{1}$$

The above process yields the normalized monthly average runoff and river structure information for each sub-basin at 120-time steps (120 months from 2013 to 2022).

2.3 Stationarity testing of the normalized runoff time series

The stationarity of the normalized runoff time series can be examined using the unit root test. A unit root is a concept in time series analysis that refers to the presence of non-stationarity in a time series variable. Specifically, if a time series has a unit root, it shows that the mean and variance of the series do not remain constant over time, showing trends or drift (Perron, 1988). The Augmented Dickey-Fuller (ADF) test is a commonly used unit root test method to find whether a time series has a unit root, thereby assessing the stationarity of the time series (Dickey et al., 1979). Specifically, for the normalized runoff time series R of each sub-basin obtained in the earlier section, a first-order autocorrelation regression analysis is conducted:

$$R_t = c + \phi \times R_{t-1} + \varepsilon_t \tag{2}$$

R_t and R_{t-1} are the observed values of the time series, representing the normalized runoff at time t and t−1 respectively. The variable c is the constant term. The coefficient ϕ is the lag term. ε_t refers to the white noise error, which follows a normal distribution with a mean of 0 and a standard deviation of 1, randomly generated. The next step is to calculate the standard error of the estimated coefficient ϕ. First, compute the residuals by subtracting the observed values from the predicted values of the autoregressive model. Then, calculate the variance of the residuals by summing the squared residuals and dividing them by the degrees of freedom (sample size minus the number of estimated parameters in the model). Finally, the standard error is obtained by taking the square root of the residual variance. The specific formula is

$$s = \sqrt{\frac{\sum_{t=1}^{n} \left(R_t - \widehat{R}_t\right)^2}{n-1}} \tag{3}$$

s is the standard error. R_t denotes the observed runoff, $\widehat{R}_t$ is the predicted runoff, and n is the sample size (120 in this study). Finally, a hypothesis test is conducted with the null hypothesis H_0 set as the time series having a unit root. The ADF statistic is calculated using the standard t-test:

$$\text{ADF} = \frac{\phi - 1}{s} \tag{4}$$

The significant level of the test is set to 0.05. By looking up the critical value for the t-test with 119 degrees of freedom at this significance level, we find it to be −2.8865. The ADF statistic is compared with the critical value. If the ADF statistic is smaller than the critical value, the null hypothesis H_0 can be rejected, indicating that the normalized runoff time series R does not have a unit root and is stationary. Conversely, if the ADF statistic is greater than the critical value, it is concluded that the normalized runoff time series does not show stationarity.

2.4 Spearman correlation analysis of runoff and river structure parameters

Spearman correlation analysis is a non-parametric statistical method used to evaluate the monotonic relationship between two variables (Zar, 2005). The analysis uses raw data including 120 normalized monthly average runoff values for each sub-basin, as well as river network density and Dist Sink. River network density refers to the length of rivers per unit area of the basin. Dist Sink is the distance from polygon outlet to the next downstream sink along the river network, in kilometers. This distance is measured to the next downstream endorheic sink (if there is one) or (if there is none) to the most downstream sink (i.e., the ocean). We perform Spearman correlation analysis between the normalized runoff for each month of all sub-basins within each large basin (with the same Pfafstetter code's first three digits) and the corresponding river network density and Dist Sink. The calculation formula is as Eq. (5).

$$r = 1 - \frac{6\sum_{i=1}^{m} d_i^2}{m(m^2 - 1)} \tag{5}$$

r is the Spearman correlation coefficient. d_i is the rank difference between the runoff data of the i-th sub-basin and the corresponding river structure parameters (river network density or Dist Sink). Rank difference refers to the difference between runoff and river structure parameters after converting them into grades (from 1 to m) by sorting them in order of magnitude. m is the number of sub-basins corresponding to each large basin. The procedure yields Spearman correlation coefficients between the normalized runoff and river network density, as well as Dist Sink, for each large basin's 120-time steps.

Next, hypothesis testing is conducted using Spearman correlation coefficient and sample size m. The null hypothesis H_0 states that the correlation coefficient equals zero, indicating no correlation between the two variables. The standard error is

$$s = \sqrt{\frac{1 - r^2}{m - 2}} \tag{6}$$

s is the standard error. The standardized statistic for Spearman's correlation coefficient is

$$t = \frac{r}{s} \tag{7}$$

t is the standardized statistic, which follows a t-distribution. Setting the significance level of the test to 0.05, if the calculated value is less than 0.05, the null hypothesis can be rejected, showing that the observed correlation coefficient is statistically significantly different from zero. Conversely, if the value is greater than or equal to 0.05, it is concluded that there is no significant correlation between the statistical variables.

2.5 Variance analysis of runoff and river orders

The variance analysis is conducted on the normalized runoff and river orders. Variance analysis is a statistical method used to compare whether there are significant differences in means among two or more groups. It evaluates whether the differences between groups exceed the level of random error by decomposing the total variance into within-group variance and between-group variance (St, L et al., 1989). The analysis uses raw data including 120 normalized monthly average runoff values for each sub-basin, as well as the river orders. The indicator of river order follows the classical ordering system: order 1 represents the main stem river from sink to source; order 2 represents all tributaries that flow into a 1st order river; order 3 represents all tributaries that flow into a 2nd order river; etc. The raw data categorizes rivers into six orders, and each region's sub-basins are divided into six groups based on these orders. For each time step, the sum of squares between groups (SSA) and the sum of squares within groups (SSE) are calculated, and the F-statistic is computed:

$$\mathrm{SSA} = \sum_{i=1}^{k} n_i \left(\overline{R_i} - \overline{\overline{R}}\right)^2 \tag{8}$$

$$\mathrm{SSE} = \sum_{i=1}^{k} \sum_{j=1}^{n_i} \left(R_{ij} - \overline{R_i}\right)^2 \tag{9}$$

$$F = \frac{\mathrm{SSA}/(k-1)}{\mathrm{SSE}/(n-k)} \tag{10}$$

where k is the number of groups. n_i is the number of sub-basins corresponding to the i-th group in each region. $\overline{R_i}$ is the average runoff depth of the corresponding sub-basins in the i-th group of each region. $\overline{\overline{R}}$ is the average runoff depth of all sub-basins in each region. R_{ij} is the runoff depth of sub-basin j in the i-th group of each region. n is the total number of sub-basins in each region. The F-statistic follows an F-distribution with (k–1, n–k) degrees of freedom. A hypothesis test is performed with the null hypothesis H_0 saying that there is no significant difference between the groups. The significance level is set at 0.05, and the critical F-value is obtained and compared with the calculated F-statistic. If the calculated F-statistic is greater than the critical F-value, the null hypothesis H_0 is rejected, showing the presence of significant differences between the groups. Conversely, if the calculated F-statistic is less than or equal to the critical F-value, it is concluded that there are no significant between-group differences in the runoff data.

3 Results

3.1 The stationarity of global normalized runoff time series

To conduct a comparative analysis of sub-basin runoff data from large river basins around the world and explore their relationship with river structure and river order, this study employed a normalization approach within each basin to process the runoff time series. On the one hand, this way helps cut some of the runoff differences caused by variations in precipitation and evaporation among regions, thus reflecting the consistency of regional changes within large basins. On the other hand, we hope to mitigate temporal variability in runoff, allowing for a more pronounced association between runoff and the non-temporal river structure and river order. Therefore, it is necessary to assess the stationarity of the time series to figure out if the normalized runoff still shows significant temporal variability.

Figure 2 shows the results of the analysis on the stationarity of global normalized runoff time series. Coastal river basins exhibit significant stationarity, such as the eastern and southern parts of Asia, coastal regions of Siberia, the entire Australasia, the Arctic, as well as coastal areas of Europe, the Middle East, Africa, North America, Central America, and South America. This is partly attributed to the strong regulatory effect of the oceans on the climate of coastal regions, resulting in relatively stable precipitation and evaporation throughout the year (Hoegh-Guldberg et al., 2019). Within each region, river basins with a wide range of spans show weaker time series stationarity, such as western Asia, central Africa, and central North America. However, overall, large basins within each region show good stationarity. Consider a ratio exceeding 50% as an indicator of consistent stationarity in the normalized runoff time series of river basins. As shown in Table 1, among the 14 large river basins in Arctic, 13 of them exceed the 50% threshold (proportion of 93%). In North and Central America, out of the 27 large river basins, 26 of them exceed the 50% threshold (proportion of 96%). In Asia, out of the 41 large river basins, 38 of them exceed the 50% threshold (proportion of 93%). In Australasia, out of the 27 large river basins, 25 of them exceed the 50% threshold (proportion of 93%). For Siberia, 12 out of the 15 large river basins, and for Africa, 26 out of the 31 large river basins exceed the 50% threshold, with proportions of 80% and 84% respectively. South America, Europe, and the Middle East exhibit weaker

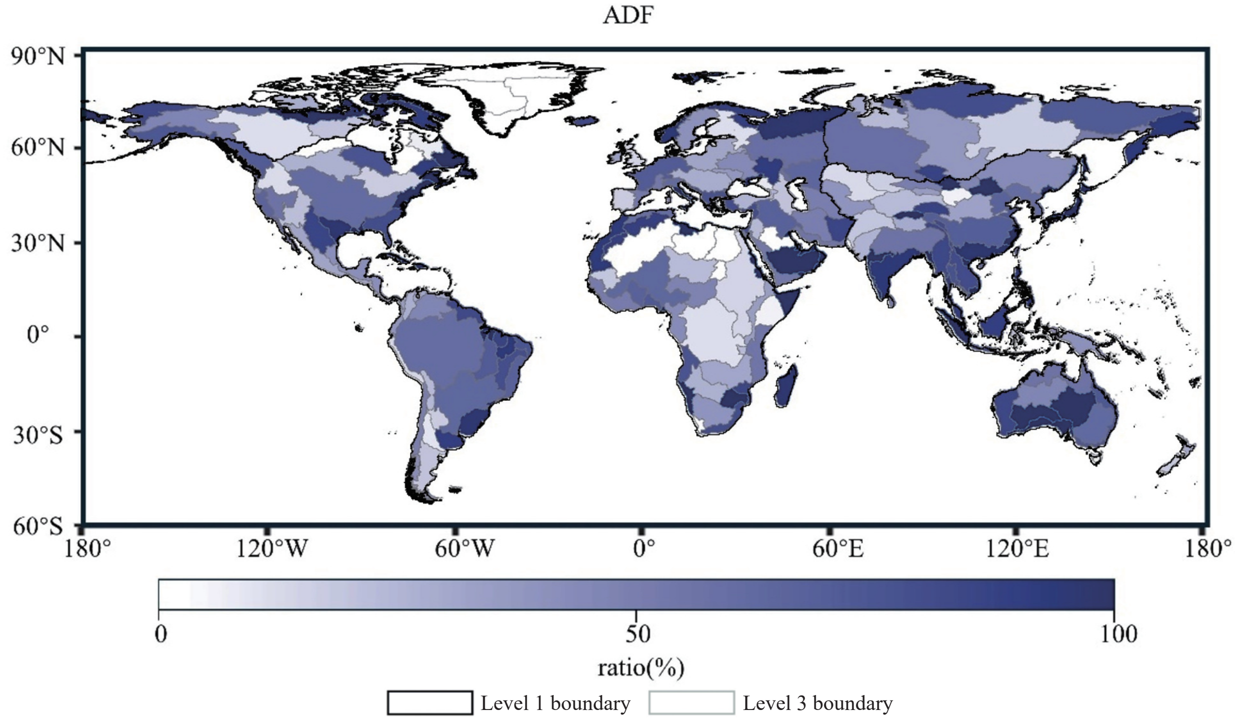

Fig. 2 Spatial distribution of stationarity ratios of large river basins. Each large river basin includes all sub-basins with the same first three digits of the Pfafstetter code. The shaded color of each large river basin is the ratio of the number of sub-basins with time series stationarity to the total number of sub-basins within the large basin.

stationarity in the large river basin runoff time series. Among the 29 large river basins in South America and the 43 large river basins in Europe and the Middle East, only 21 and 32 basins respectively exceed the 50% threshold, with proportions of 72% and 74%.

The stationarity of runoff time series in African and Middle East large river basins is mainly influenced by arid climate, with scarce precipitation and high evaporation, leading to significant instability and substantial regional variations (Hulme et al., 2001; Lelieveld et al., 2012). The stationarity of runoff time series in South American large river basins is mainly affected by the Southern Oscillation events (Grimm, 2011). It can also be seen from Figure 1 that the unstable regions are primarily found in the western Pacific coastal areas. However, the runoff time series in the region influenced by the South Atlantic convergence zone still show good stationarity, which reflects the regional consistency of normalized runoff time series. In Siberia, the stationarity of runoff time series is weaker. Considering the good stationarity of runoff time series in the Arctic region, the high latitudes are not the main cause for this phenomenon (Roots, 1989). This could be attributed to the poorer regional consistency within the large river basins of Siberia. In Europe, human activities influence the distribution of water resources to a large extent. Regional differences in this influence reduce the stationarity of runoff time series within large river basins (Vörösmarty et al., 2010).

From the perspective of sub-basins, the analysis of the normalized runoff time series stationarity can also be conducted for river basins on each region. As shown in Table 2, in Asia, out of 6,365 small sub-basins, 5,371 exhibit time series stationarity in runoff, accounting for 84% of the total. In Australasia, out of 2,257 small sub-basins, 1,969 exhibit time series stationarity in runoff, accounting for 87%. The higher proportions of stationary sub-basins align with the results obtained from the analysis of large river basins. For the Arctic region, out of 1,923 sub-basins, 1,409 exhibit time series stationarity in runoff, accounting for 73%. In North and Central America, out of 5,395 sub-basins, 4,244 show time series stationarity in runoff, accounting for 79%. The proportions of stationary sub-basins in these two regions are slightly lower compared to the analysis of large river basins. In Europe and the Middle East, out of 4,969 sub-basins, 3,498 exhibit time series stationarity in runoff, accounting for 70%. In Siberia, out of 4,368 small sub-basins, 3,143 show time series stationarity in runoff, accounting for 72%. The lower proportions of stationary sub-basins align with the results obtained from the analysis of large river basins. In Africa, out of 4,540 sub-basins, only 2,456 have time series stationarity in runoff, accounting for the lowest proportion of 61%. In contrast, in South America, out of 5,542 sub-basins, 4,643 exhibit time series stationarity in runoff, accounting for a higher proportion of 84%. The contrasting results between the two regions reflect the differences in their river basin structures. In Africa, large river basins with a larger number of sub-basins show poorer consistency in their structure. This is because under arid conditions, the differences in basin structure contribute to the increased differences in runoff between regions. Conversely, in South America, large river basins with a greater number of sub-basins show better consistency in their structure. This shows that the complex basin structures, influenced by monsoon climates and abundant extreme precipitation events, help regulate the distribution of runoff within the river basins. This also explains the phenomenon mentioned earlier of the better stationarity of runoff time series in the region influenced by the South Atlantic Convergence Zone.

In summary, normalization can cut some of the runoff differences caused by regional precipitation and evaporation disparities, reflecting the consistency of regional variations within large river basins. Additionally, normalization helps reduce the temporal variability of runoff sequences.

https://doi.org/10.26599/HYD.2023.9380005.VR

3.2 Correlation between global normalized runoff and river structure

For each region's data, correlation analysis was conducted between normalized runoff and river network density as well as Dist Sink. The temporal variation of correlation was seen to reflect the level of correlation and consistency between normalized runoff and river structural parameters in different basins. Spearman correlation analysis was used to effectively assess the correlation between two non-normally distributed continuous variables.

Figure 3 reflects the significance of the correlation between global normalized runoff and river network density as well as Dist Sink. From the figure, the significance of the correlation between normalized runoff and river network density or Dist Sink varies across different regions in large river basins worldwide. Regarding river network density, a strong correlation with normalized runoff is clear in the southern region of the Arctic, Central and North America, northern parts of South America, western and eastern Europe, coastal areas of southern and northern Africa, most parts of Asia and Siberia, and the northern region of Australasia. As for Dist Sink, a strong correlation with normalized runoff is observed in the southern region of the Arctic, central North America, Central America, eastern South America, western and eastern Europe, coastal areas of southern and northern Africa, most parts of Asia, the southern region of

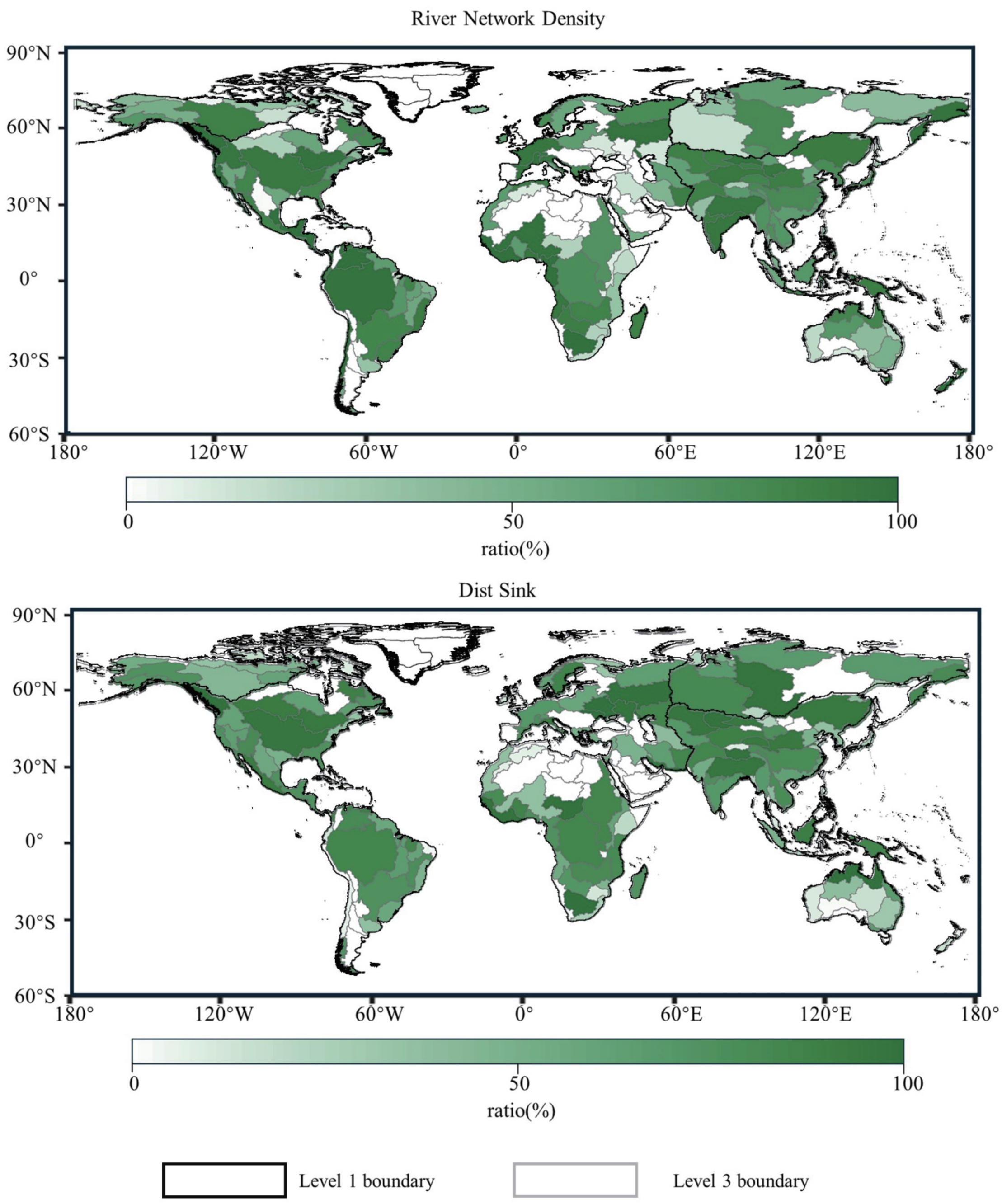

Fig. 3 Spatial distribution of the significant correlation ratio between normalized runoff and river network density, and Dist Sink in large river basins. Each large river basin includes all sub-basins with the same first three digits of the Pfafstetter code. The color of the basins reflects the ratio of data with a significant non-zero correlation (*p*-value less than 0.05) in the time series.

Siberia, and the northern region of Australasia. The distribution of significance in the correlation between normalized runoff and river network density or Dist Sink is not consistent across large river basins worldwide.

Considering a threshold of more than 50% as a statistical criterion, it is believed that there is a significant correlation between normalized runoff and river structure in basins where the ratio exceeds 50%. Regarding river network density, among the 45, 29, and 31 major basins in Asia, North America and Central America, and South America respectively, there are 29, 16, and 17 basins with a ratio exceeding 50%, accounting for 64%, 55%, and 55% respectively. The relatively high ratios indicate a consistent and significant correlation between normalized runoff and river network density in these regions. However, in Africa, the Arctic, Australasia, Europe and the Middle East, and Siberia, among the 49, 19, 47, 50, and 18 major basins respectively, only 14, 3, 12, 15, and 6 basins have a ratio exceeding 50%, accounting for 29%, 16%, 26%, 30%, and 33% respectively. This suggests that in these regions, the correlation between normalized runoff and river network density is not consistently significant. Like the analysis of river network density, for Dist Sink, in the 45, 29, and 31 major basins in Asia, North America and Central America, and South America respectively, there are 59, 20, and 15 basins with a ratio exceeding 50%, accounting for 56%, 69%, and 48% respectively. However, in Africa, the Arctic, Australasia, Europe and the Middle East, and Siberia, among the 49, 19, 47, 50, and 18 major basins respectively, only 16, 6, 5, 18, and 7 basins have a ratio exceeding 50%, accounting for 33%, 32%, 11%, 36%, and 39% respectively. The regions that show significant correlations between river network density, Dist Sink, and normalized runoff are the same.

Figure 4 depicts the correlation between normalized runoff and river network density, as well as Dist Sink, within large river basins across different regions. The correlation values in the figure represent the average correlation over 120-time steps for each large river basin. Overall, the correlation between normalized runoff and river structure parameters does not show consistent patterns within large river basins across regions. Regarding river network density, in the southern Arctic, it shows a negative correlation with normalized runoff. In North America, Central America, and South America, the correlation is generally positive, with strong correlations observed along the coastal areas of Central America, western North America, and South America. The Pacific Ocean brings abundant precipitation to these

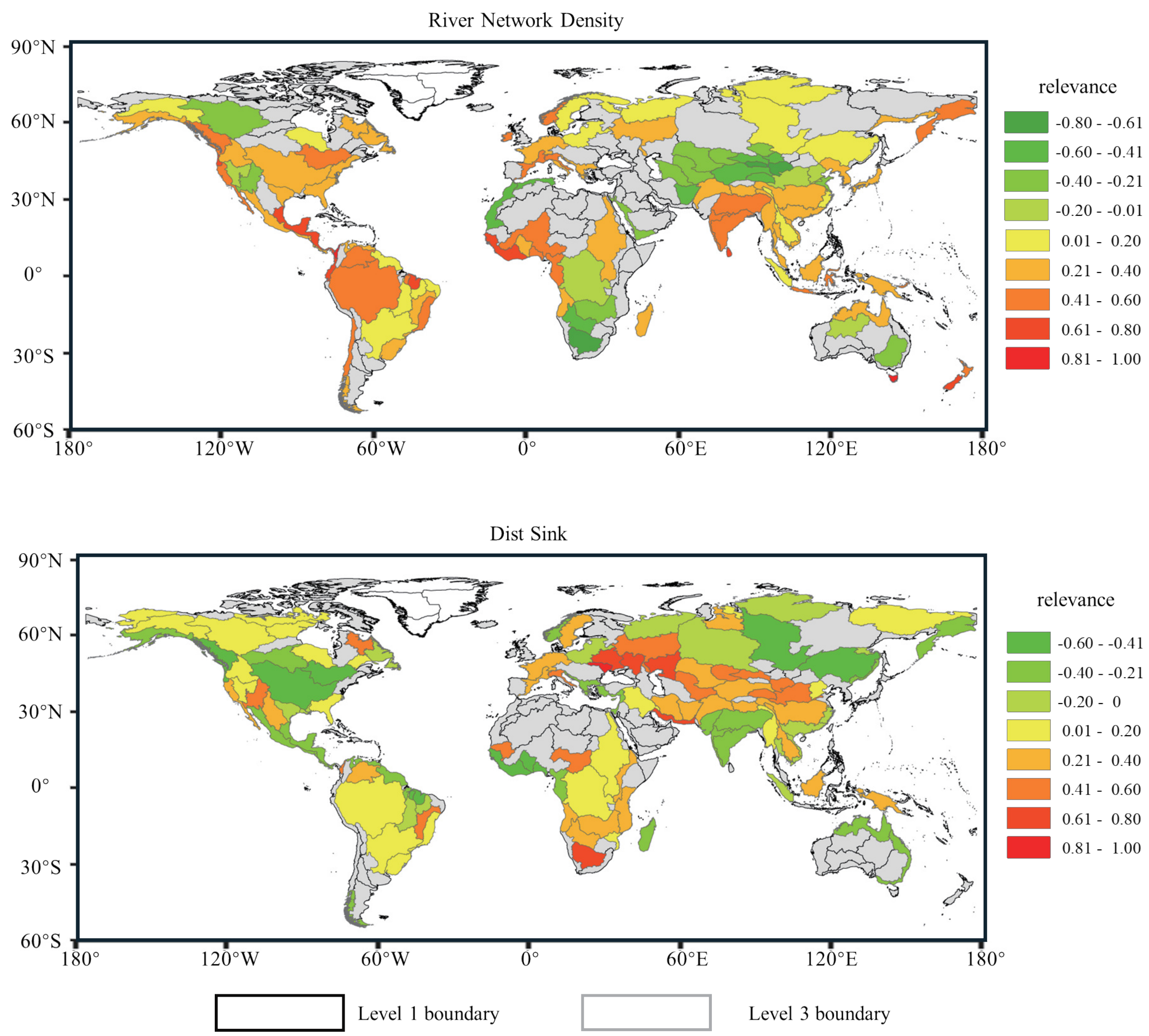

Fig. 4 Spatial distribution of the correlation between normalized runoff and river network density, and Dist Sink in large river basins. Each large river basin includes all sub-basins with the same first three digits of the Pfafstetter code. The color of the basins reflects the correlation between normalized runoff and river network density, as well as Dist Sink. Regions with non-significant correlations are represented in gray, showing that their correlations were not calculated.

 https://doi.org/10.26599/HYD.2023.9380005.VR

regions, leading to synchronous increases in both river network density and runoff, thereby mutually reinforcing each other. A similar pattern is seen in the western part of Africa, western Europe, southern Asia, and island regions in Australasia. In most inland regions such as the southern part of the Arctic, southern Africa, northern Asia, the Middle East, and central Oceania, there is a significant negative correlation between river network density and normalized runoff. In inland regions, a higher river network density accelerates the outflow of runoff, causing it to be transported more quickly out of the river basin. As for Dist Sink, it is found to have an opposite correlation with normalized runoff compared to river network density. This is because in coastal basins, sub-basins closer to the coast tend to receive more precipitation, resulting in more runoff and smaller Dist Sink values. In inland basins, on the other hand, larger Dist Sink values show that the corresponding sub-basins are closer to the source of the river, where the runoff is typically greater.

Figure 5 illustrates the standard deviation of the correlation between normalized runoff and river network density, as well as Dist Sink, within each region's large river basins. The standard deviation values in the figure represent the standard deviation of the correlations over 120-time steps for each large river basin, reflecting the fluctuation of the correlations. Overall, the standard deviation of the correlation between normalized runoff and river structure parameters within large river basins is not consistent across regions. For river network density and Dist Sink, their correlations with normalized runoff show larger standard deviations in the eastern coastal regions of North America and South America, the northern coastal regions of Europe and Siberia, and the eastern and southeastern coastal regions of Asia. This shows significant variability in the correlations within these regions, without a consistent trend.

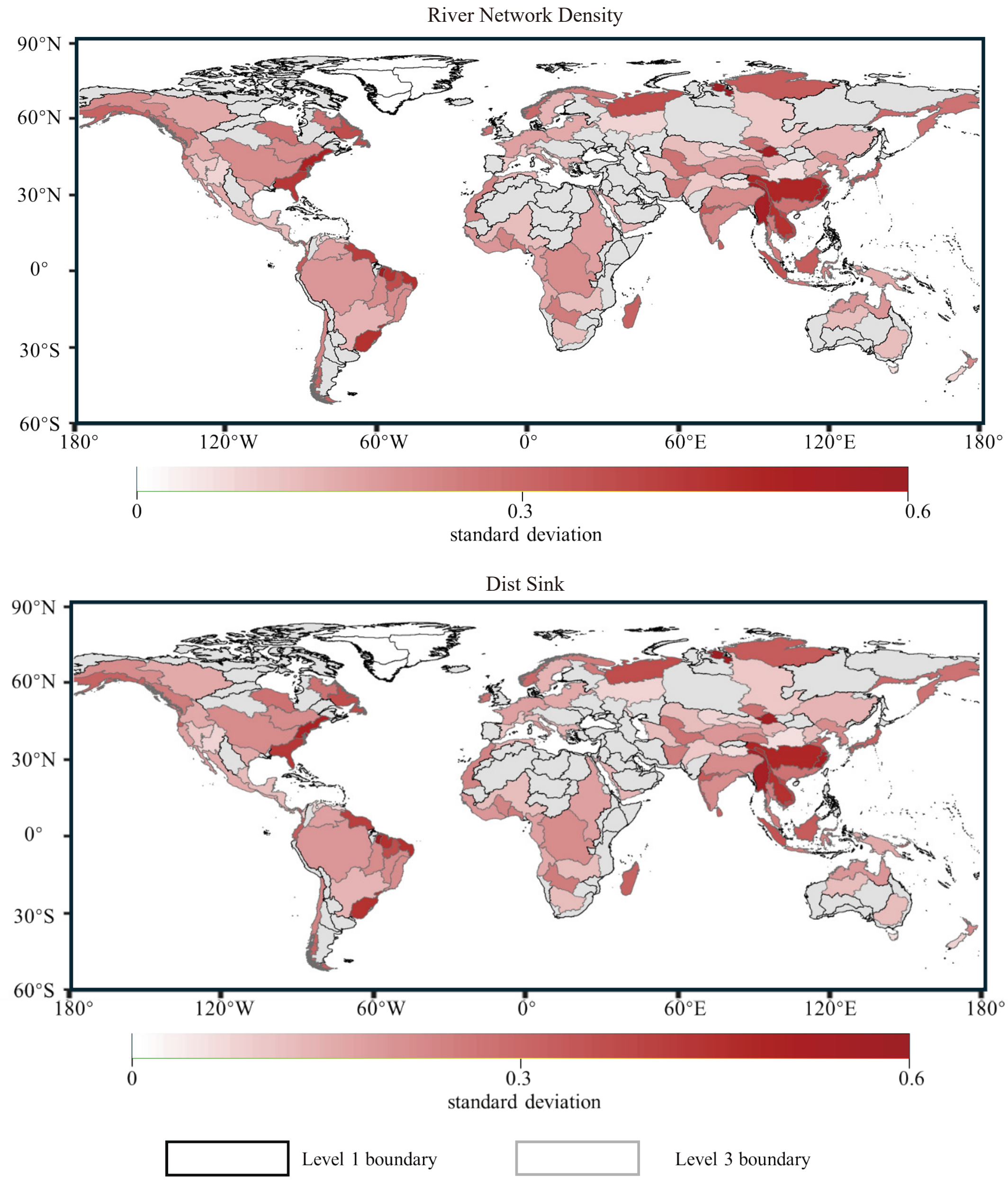

Fig. 5 Spatial distribution of the standard deviation between normalized runoff and river network density and Dist Sink, in large river basins. Each large river basin includes all sub-basins with the same first three digits of the Pfafstetter code. The color of the basins reflects the size of the standard deviation about correlation between normalized runoff and river network density, as well as Dist Sink. Regions with non-significant correlations are represented in gray, showing that their correlations were not calculated.

3.3 The variation of global normalized runoff across river orders

For each region, analysis of variance can assess whether there are differences in normalized runoff among different river orders within each sub-basin. As shown in Table 3, sub-basins in Africa, Asia, North America, and Siberia show significant differences in normalized runoff across different river orders, and these differences are consistent over time. In South America, normalized runoff in different river orders only shows no significant differences in three-time steps. In Australasia, Arctic and Europe, sub-basins show no significant differences in normalized runoff across different river orders in 16-, 17-, and 14-time steps respectively, accounting for 13%, 14%, and 12%.

In Figure 6, we observed variations in normalized runoff across different river orders. Generally, 1- and 2-order rivers exhibited higher average normalized runoff, except for zero-order rivers. Zero-order refers to conglomerates of small coastal watersheds. A higher average normalized runoff implies that sub-basins within these larger river basins tend to experience greater runoff depths more frequently. This pattern is particularly evident in South America and least prominent in North America. Although the number of 4-order rivers is limited in Australasia, some of these rivers exhibit high mean normalized runoff, indicating relatively higher runoff within their corresponding sub-basins in the larger basin. In Africa, the Arctic, and Australasia, 5-order rivers exhibited relatively lower mean normalized runoff.

Overall, there are significant differences in normalized runoff among different river orders in each region, and further analysis is needed to understand the correlation between river orders and normalized runoff.

Table 1 Stationarity analysis at large basin scale across global regions. The regions include Europe and the Middle East (EU), Asia (AS), Australasia (AU), Africa (AF), North America and Central America (NA), South America (SA), Antarctica (AR), and Siberia (SI).

Region	Total Large Basins	Basins >50% Stationary	Proportion (Large Basin)
AR	14	13	93%
NA	27	26	96%
AS	41	38	93%
AU	27	25	93%
SI	15	12	80%
AF	31	26	84%
SA	29	21	72%
EU	43	32	74%

Table 2 Stationarity analysis at sub-basin scale across global regions. The regions include Europe and the Middle East (EU), Asia (AS), Australasia (AU),Africa (AF), North America and Central America (NA), South America (SA), Antarctica (AR), and Siberia (SI).

Region	Total Large Basins	Basins >50% Stationary	Proportion (Large Basin)
AR	1,923	1,409	73%
NA	5,395	4,244	79%
AS	6,365	5,371	84%
AU	2,257	1,969	87%
SI	4,368	3,143	72%
AF	4,540	2,456	54%
SA	5,542	4,643	84%
EU	4,969	3,498	70%

Table 3 Table of the number of months and percentage of months with variances for each region of the globe. The regions include Europe and the Middle East (EU), Asia (AS), Australasia (AU), Africa (AF), North America and Central America (NA), South America (SA), Antarctica (AR), and Siberia (SI).

Region	Number of months with variances	Percentage of months with variances
EU	106	88%
SA	117	98%
SI	120	100%
AR	103	86%
AF	120	100%
AS	120	100%
AU	104	87%
NA	120	100%

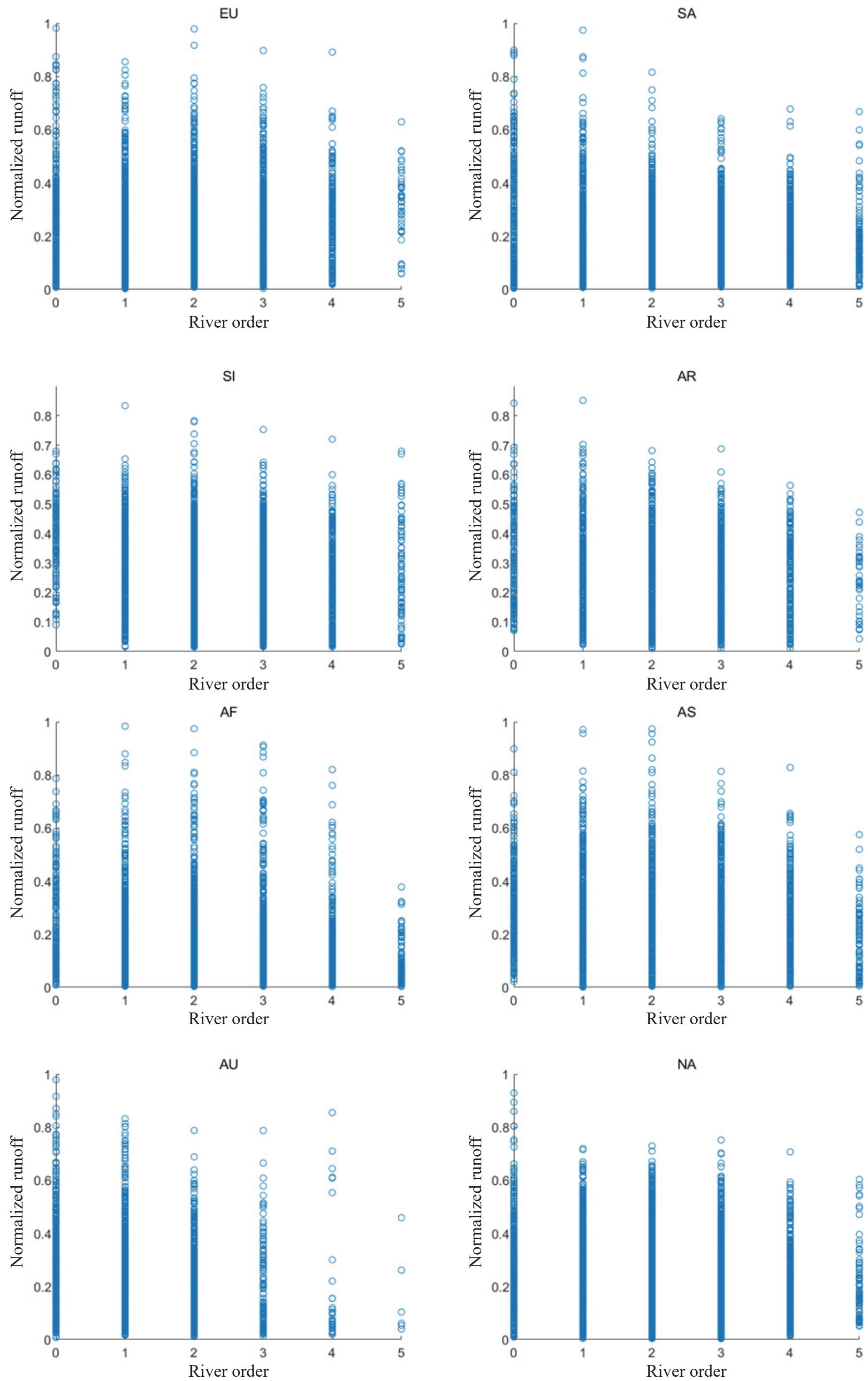

Fig. 6 Scatterplots of river order and average normalized runoff for sub-basins in each region of the world. The abscissa and ordinate represent river orders and average normalized runoff, respectively. The regions include Europe and the Middle East (EU), South America (SA), Siberia (SI), Antarctica (AR), Africa (AF), Asia (AS), Australasia (AU) and North America and Central America (NA). The average normalized runoff for each sub-basin is obtained by averaging the normalized runoff for each month.

4 Conclusions and implications

This study systematically analyzed the spatiotemporal patterns of normalized runoff across global river basins and investigated its relationships with river structure parameters and river orders through stationarity testing, correlation analysis, and variance analysis. The key findings and their implications are summarized as follows.

First, normalized runoff exhibits temporal stationarity across most global river basins, with over 70% of sub-basins in most regions showing stationary time series. This validates that within-basin normalization successfully reduces temporal variability caused by climate fluctuations while preserving spatial patterns related to basin structural characteristics. Regions with lower stationarity (Africa: 54%, Europe and Middle East: 70%) reflect the influence of arid climates with high spatial variability and extensive human water management activities. The differences in stationarity distribution within regions demonstrate how basin structure affects regional consistency, providing a suitable foundation for comparative analysis of blue water distribution across heterogeneous river systems.

Second, the relationship between normalized runoff and river structure parameters exhibits significant spatial heterogeneity, with fundamentally different patterns in coastal versus inland regions. In coastal regions, river network density shows positive correlations with normalized runoff, where denser networks facilitate water retention and groundwater interactions. Conversely, inland regions exhibit negative correlations, indicating that denser networks accelerate runoff evacuation in water-limited environments. Distance to sink (Dist Sink) shows opposite patterns, reflecting different hydrological mechanisms. This spatial heterogeneity has important management implications: strategies must be region-specific, with coastal basins benefiting from enhanced river network connectivity while inland basins requiring optimized network configuration rather than simply increased density. The substantial temporal variability in some coastal regions indicates that structure-runoff relationships can vary seasonally or interannually in climatically variable areas.

Third, river orders significantly influence normalized runoff distribution, with orders 1 and 2 (main stems and primary tributaries) consistently exhibiting higher average normalized runoff than higher-order tributaries. This pattern is most pronounced in South America and least evident in heavily modified North American systems. These findings challenge traditional assumptions that focus primarily on main stem discharge and suggest that tributary systems contribute more substantially to total blue water availability than currently recognized. This has practical implications: monitoring programs should expand tributary coverage, and water availability estimates based solely on main stem gauging may systematically underestimate renewable blue water resources.

The demonstrated correlations between river structure and blue water distribution establish a foundation for improved resource assessment and management. The readily-available structural parameters (river network density, distance to sink, river order) can serve as useful predictors for estimating spatial patterns of water availability, particularly in data-scarce regions. However, several areas require further investigation. Future research should employ process-based hydrological modeling to elucidate causal mechanisms underlying structure-runoff relationships and quantify the relative importance of climate, geology, and human activities. Extending analyses to multi-decadal timescales would better capture long-term climate variability not evident in the current 10-year period. Incorporating anthropogenic factors such as reservoir operations and land use changes would provide more complete understanding in heavily managed systems. Developing predictive models integrating river structure parameters with climate projections would enable forecasting under future scenarios, supporting adaptive water resource planning. By revealing how river network density, distance to sink, and river order shape runoff patterns, this work provides practical guidance for developing region-specific water management strategies that account for the distinctive hydrological characteristics of different geographical settings under global environmental change.

Data availability

The data that support the findings of this study are derived from publicly available datasets:
Source datasets:
- River basin delineations: HydroBASINS v1.0 (Lehner & Grill, 2013), available at https://www.hydrosheds.org
- River network data: HydroRIVERS v1.0 (Lehner & Grill, 2013), available at https://www.hydrosheds.org
- Runoff data: ERA5-Land monthly averaged data (Muñoz Sabater, 2019), available at https://cds.climate.copernicus.eu

Declaration of competing interests

The authors have no competing interests to declare that are relevant to the content of this article. The author Guangqian Wang is the Editor-in-Chief of this journal. The author Deyu Zhong is the member of Acting Executive Editors of this journal.

References

Arnell, N. W. (2004). Climate change and global water resources: SRES emissions and socio-economic scenarios. *Global Environmental Change*, 14(1): 31–52.

Dickey, D. A., Fuller, W. A. (1979). Distribution of the estimators for autoregressive time series with a unit root. *Journal of the American Statistical Association*, 74: 427–431.

Döll, P., Trautmann, T., Gerten, D., Schmied, H. M., Ostberg, S., Saaed, F., & Schleussner, C. F. (2018). Risks for the global freshwater system at 1. *5 C and 2 C global warming. Environmental Research Letters*, 13: 044038.

Falkenmark, M., Rockström, J. (2006). The new blue and green water paradigm: Breaking new ground for water resources planning and management. *Journal of Water Resources Planning and Management*, 132: 129–132.

Feng, X., Fu, B., Piao, S., Wang, S., Ciais, P., Zeng, Z., Lv. Y., Zeng, Y., Jiang, X., Wu, B. (2016). Revegetation in China's Loess Plateau is approaching sustainable water resource limits. *Nature Climate Change*, 6: 1019–1022.

Grimm, A. M. (2011). Interannual climate variability in South America: Impacts on seasonal precipitation, extreme events, and possible effects of climate change. *Stochastic Environmental Research and Risk Assessment*, 25: 537–554.

Hoegh-Guldberg, O., Lovelock, C., Caldeira, K., Howard, J., Chopin, T., Gaines, S. (2019). The ocean as a solution to climate change: Five opportunities for action. Washington: World Resources Institute.

Huang, J., Yu, H., Dai, A., Wei, Y., Kang, L. (2017). Drylands face potential threat under 2 C global warming target. *Nature Climate Change*, 7: 417–422.

Hulme, M., Doherty, R., Ngara, T., New, M., Lister, D. (2001). African climate change: 1900–2100. *Climate Research*, 17: 145–168.

IPCC. (2023). Contribution of working groups I, II and III to the sixth assessment report of the intergovernmental panel on climate change sections. In: Climate Change 2023: Synthesis Report. DOI: 10.59327/IPCC/AR6-9789291691647.

Jaramillo, F., Destouni, G. (2015). Local flow regulation and irrigation raise global human water consumption and footprint. Science, 350(6265): 1248−1251. https://doi.org/10.1126/science.aad1010.

Kundzewicz, Z. W., Mata, L. J., Arnell, N. W., Döll, P., Jimenez, B., Miller, K., Oki, T., Şen, Z., Shiklomanov, I. (2008). The implications of projected climate change for freshwater resources and their management. *Hydrological Sciences Journal*, 53: 3–10.

Lehner, B., Grill, G. (2013). Global river hydrography and network routing: Baseline data and new approaches to study the world's large river systems. *Hydrological Processes*, 27: 2171–2186.

Lelieveld, J., Hadjinicolaou, P., Kostopoulou, E., Chenoweth, J., El Maayar, M., Giannakopoulos, C., Hannides, C., Lange, M. A., Tanarhte, M., Tyrlis, E., et al. (2012). Climate change and impacts in the Eastern Mediterranean and the Middle East. *Climatic Change*, 114: 667–687.

Leopold, L. B., Wolman, M. G., Miller, J. P. (1964). Fluvial Processes in Geomorphology. San Francisco: W. H. Freeman and Company.

Liu, C. M., Wang, K. W., Wang, G. (2022). Analyzing the changes of streamflow and associated influencing factors in the Yellow River Basin from 1956 to 2016. *Yellow River*, 44: 1–5.

Mekonnen, M. M., Hoekstra, A. Y. (2016). Four billion people facing severe water scarcity. Science Advances, 2(2): e1500323. https://doi.org/10.1126/sciadv.1500323.

Muñoz Sabater, J. (2019). ERA5-Land hourly data from 1950 to present. Copernicus Climate Change Service (C3S) Climate Data Store (CDS).

Oki, T., Kanae, S. (2006). Global hydrological cycles and world water resources. *Science*, 313: 1068–1072.

Olivera, F., Lear, M. S., Famiglietti, J. S., & Asante, K. (2002). Extracting low-resolution river networks from high-resolution digital elevation models. *Water Resources Research*, 38: 13–1.

Perron, P. (1988). Trends and random walks in macroeconomic time series: Further evidence from a new approach. *Journal of Economic Dynamics and Control*, 12: 297–332.

Roots, E. F. (1989). Climate change: High-latitude regions. *Climatic Change*, 15: 223–253.

Scanlon, B. R., Jolly, I., Sophocleous, M., Zhang, L. (2007). Global impacts of conversions from natural to agricultural ecosystems on water resources: Quantity versus quality. *Water Resources Research*, 43: W03437.

Shiklomanov, I. A. (2000). Appraisal and assessment of world water resources. *Water International*, 25: 11–32.

Shiklomanov, I. A., Rodda, J. C. (2003). World Water Resources at the Beginning of the Twenty-First Century. Cambridge: Cambridge University Press.

St, L., Wold, S. (1989). Analysis of variance (ANOVA). *Chemometrics and intelligent laboratory systems*, 6: 259–272.

Twidale, C. R. (2004). River patterns and their meaning. *Earth-Science Reviews*, 67: 159–218.

Verdin, K. L., & Verdin, J. P. (1999). A topological system for delineation and codification of the Earth's river basins. *Journal of Hydrology*, 218: 1–12.

Vörösmarty, C. J., McIntyre, P. B., Gessner, M. O., Dudgeon, D., Prusevich, A., Green, P., Glidden, S., Bunn, S. E., Sullivan, C. A., Liermann, C. R., et al. (2010). Global threats to human water security and river biodiversity. *Nature*, 467: 555–561.

Wang, C. Y., Shang, S. H., Jia, D. D., Han, Y. P., Sauvage, S., Sánchez-Pérez, J. M., Kuramochi, K., Hatano, R. (2018). Integrated effects of land use and topography on streamflow response to precipitation in an agriculture-forest dominated northern watershed. *Water*, 10: 633.

Zar, J. H. (2005). Spearman rank correlation. In Encyclopedia of Biostatistics, 2nd ed. Armitage, P., Colton, T., Eds. Hoboken: John Wiley.

Zhang, L., Dawes, W. R., Walker, G. R. (2001). Response of mean annual evapotranspiration to vegetation changes at catchment scale. *Water Resources Research*, 37: 701–708.